KARYA ILHAM PUBLISHING
CONNECTING MINDS, BRIDGING IDEAS, INSPIRING READERS

Malaysian Journal on Composites Science and Manufacturing

Journal homepage:
https://karyailham.com.my/index.php/mjcsm/index
ISSN: 2716-6945

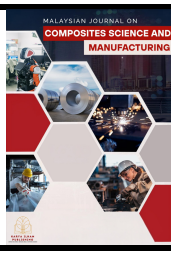

Hydrothermal Synthesis and Characterization of ZSM-5 Zeolite from Nigerian-Origin Kaolin: Effects of Crystallization Temperature on Structure and Morphology

Henry E. Mgbemere[1], Augustine B. Okoubulu[2,*], Cynthia C. Nwaeju[3,5], Pius A. Uzere[4], Francis O. Edoziuno[5]

[1] Metallurgical and Materials Engineering Department, University of Lagos, Akoka-Yaba, Lagos, Nigeria
[2] Materials and Metallurgical Engineering Department, Southern Delta University, P.M.B. 5, Ozoro, Nigeria
[3] Department of Mechanical Engineering, Nigeria Maritime University, Okerenkoko, Delta State, Nigeria
[4] Department of Mechanical Engineering, Federal University of Petroleum Resources, Effurun, Delta State, Nigeria
[5] Department of Metallurgical and Materials Engineering, Nnamdi Azikiwe University, P.M.B. 5025 Awka

ARTICLE INFO

Article history:
Received 6 January 2026
Received in revised form 20 February 2026
Accepted 1 June 2026
Available online 4 June 2026

Keywords:
ZSM-5 Zeolite, Kaolin, Crystallization, Metakaolinization, Hydrothermal synthesis

ABSTRACT

This study investigates the hydrothermal synthesis and characterization of ZSM-5 zeolite from Ajebo kaolin in Nigeria, with a focus on the effects of crystallization temperature on the structure and morphology. ZSM-5 zeolite was synthesized at crystallization temperatures of 100°C, 120°C, and 150°C, with a fixed crystallization time of 6 hours. Characterization techniques, including XRF, FTIR, XRD, EDX, and SEM, were employed to analyze the composition and structure of the synthesized zeolites. The results confirmed the synthesis of ZSM-5 at all temperatures, with the sample crystallized at 150°C achieving the highest crystallinity (85%) and a distinct hexagonal prismatic morphology. XRF analysis revealed high SiO_2 (50–60%) and Al_2O_3 (40–45%) content. FTIR analysis confirmed the absence of -OH vibrations (3600–3700 cm^{-1}) in metakaolin, indicating successful dihydroxylation. A prominent peak at 1078 cm^{-1} validated the formation of ZSM-5. XRD patterns substantiated the phase transformation from kaolin to ZSM-5, with improved crystallinity at higher temperatures. SEM images showed that the ZSM-5 synthesized at 150°C exhibited well-defined hexagonal prisms. The higher the crystallization temperature, the better the crystallinity of the synthesized zeolites. This study demonstrates Ajebo kaolin as a sustainable and cost-effective source for producing ZSM-5 zeolite, highlighting its potential applications as a catalyst in the breakdown of hydrocarbons and other industrial processes.

1. Introduction

Zeolite is a crystalline aluminosilicate mineral that forms naturally through the interaction of volcanic ash with alkaline water [1-3]. The name “ZEO” is derived from two Greek words: “zeo,” meaning to boil, and “lithos,” meaning stone. Zeolites possess three-dimensional structures arising from oxygen-linked frameworks of [SiO4]4− and [AlO4]5− polyhedral [4,5]. The lattice structure of

* *Corresponding author.*
E-mail address: okoubulua@gmail.com

zeolites carries a net negative charge, enabling them to attract and bind various cations, including sodium, lead, manganese, and zinc. They are porous crystals with the structural formula expressed as Mx/n [(Al2O3)x(SiO2]y.wH2O, where M represents metal cations external to the framework and n denotes their valence states. The parameters x and y correspond to the number of aluminum and silicon tetrahedra, while 'w' indicates the number of water molecules present [6-8]. The formation of zeolite is suggested to be significantly influenced by several parameters, including batch composition, silica-to-alumina ratio, presence of organic templates, water content, aging time, temperature, pH, and crystallization duration [9,10]. Among these factors, crystallization temperature plays a crucial role in the synthesis of zeolites. It can affect various aspects such as growth velocity, the interface reactions between different crystal faces or directions, and the diffusion rate of active crystal particles [11-13].

Zeolites are produced on a large scale, often synthesized using costly chemical reagents [3,14]. Due to the high production costs, researchers have investigated more affordable materials as precursors for zeolite synthesis. Previous research has shown that scientists have investigated low-cost and effective alternative materials, including kaolin, rice husk, fly ash, municipal solid waste, industrial sludge, coal ash, clay minerals, and volcanic glasses, as substitutes for chemical reagents in zeolite production [15-19]. The well-known, industrially significant zeolite is ZSM-5, which is known for its ability to catalyse a variety of reactions due to its exceptional physicochemical properties [14]. These features, exceptionally high stability, selectivity, and sensitivity, significantly influence its catalytic reactions. Formerly synthesized in 1971 by Argauer and Landolt [20], ZSM-5 has found widespread applications in industries such as petroleum refining, chemical production, and gas separation. It catalyzes processes such as isomerization, alkylation, and hydrocarbon conversion and can also function as a bifunctional catalyst when combined with metals or acids. Traditional ZSM-5 synthesis often involves the use of chemicals that can potentially pose environment and health risk [21,22]. Therefore, exploring alternative, more sustainable materials to replace these chemicals is crucial for making the production process more cost-effective and environmentally friendly.

The natural minerals obtained from alternative materials differ in their chemical, processing, and mineralogical compositions, which may significantly affect the final product of zeolites when used as precursors. Rice husk, known for its high silica content and the presence of palygorskite, can be converted into highly siliceous ZSM-5. However, investigations by Jiang et al. [18], and Panpa and Jinawath [17] revealed that the addition of aluminum to reduce the Si/Al ratio had an unfavorable effect on the formation of ZSM-5 from palygorskite. Chareonpanich et al. [23] found that fly ash was a feasible source for zeolite synthesis. However, the synthesis process requires high temperatures exceeding 200°C. Despite this, when using fly ash as a precursor, only low yields are obtained due to the limitations posed by the temperature range. Among these materials, kaolin has been studied as a potential alternative to chemical reagents [5,10]. However, the composition and structure of kaolin vary significantly depending on its geographic origin and formation process. These variations in composition and structure can influence its chemical reactivity during synthesis [24,25]. Kaolin has a layered structure with the chemical composition $Al_2Si_2O_5(OH)_4$. Its primary constituent, kaolinite, is characterized by a unique structural arrangement of alternating alumina octahedral sheets and silica tetrahedral sheets. It shares a similar silicon-to-aluminum (Si/Al) ratio with zeolites, making it a potential candidate for zeolite synthesis [24,25]. These layers are interconnected, where the tips of the silica tetrahedrons share a standard layer with adjacent octahedral sheets, as illustrated in Fig. 1

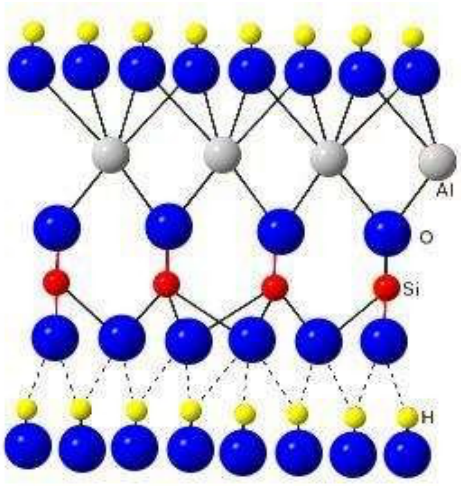

Fig. 1. Layered structure of kaolinite [26]

Kaolin minerals are abundant worldwide. When heated, crystalline kaolin transforms into an amorphous solid through a process called metakaolinization or dehydroxylation. The amorphous kaolinite is highly reactive, exhibiting a metastable phase that can be easily converted into zeolite [27,28]. The thermal treatment of kaolinite and the hydrothermal reaction of metakaolin are two major steps required to obtain zeolite from kaolin [10]. During the process, metakaolin reacts with an aqueous alkali medium, leading to the formation of the zeolite structure. The reactivity of metakaolin is influenced by temperature, composition, and morphology. Studies have shown that metakaolin reaches its maximum calcination between 750-800°C [29,30]. Recently, researchers have focused on exploring the reaction mechanism and optimizing the reaction conditions for synthesizing ZSM-5 zeolites using metakaolinized kaolin. Factors such as crystallization temperature, SiO_2-to-water ratio, aging duration, and crystallization time have been identified as key influences on crystal growth during zeolite synthesis [30,31].

A comparison has been made between the leaching of kaolin and Bolivian diatomaceous earth in the synthesis of ZSM-5 zeolite. A longer induction time was observed while small amounts of Mordenite were also formed [32]**.** Indonesian kaolin has been used to produce ZSM-5 without converting to metakaolin using sodium fluoride, and the use of NaOH led to the formation of amorphous and other crystalline materials [33]. ZSM-5 has been synthesized directly from Bangka kaolin with the aid of ZSM-5 seed as a structure-directing agent (SDA) and aging while adding additional silica to control the Si/Al ratio [34]. With a structure-directing agent using a kaolin source, a one-pot non-template synthesis of ZSM-5 has been achieved, where NaOH acts as a desilication agent after the formation of the zeolite [35,36]**.** The effects of kaolin content, crystallization Time, and temperature on the size and crystallinity of the products have been investigated. It was observed that increasing the kaolin content was more effective in increasing crystal size at higher crystallization temperatures and times [37]. A high content of quartz was observed in the synthesized ZSM-5 [1].

Although Nigeria has abundant kaolin deposits, research on synthesizing ZSM-5 zeolite from locally sourced kaolin and the impact of different synthesis parameters remains limited. This study focuses on the hydrothermal synthesis and characterization of ZSM-5 zeolite using kaolin from Ajebo, Nigeria. This research explores the hydrothermal synthesis and characterization of ZSM-5 zeolite derived from Nigerian kaolin. The objective of this study is to investigate the effect of crystallization temperature and minimum time on the properties of ZSM-5 zeolites.

2. Materials and Methods

2.1 Sample Preparation

In this study, kaolin sourced from Ajebo in Ogun State, Nigeria, was used as the alumina source material, as illustrated in Fig. 2. Other materials utilized include sulfuric acid (H_2SO_4), hydrochloric acid (HCl), distilled water, external silica (Ludox AS-40 colloidal), and sodium hydroxide (NaOH) pellets with 97% purity. The kaolin served as the precursor for zeolite synthesis. The kaolin was first crushed using a tumbler mill and mixed with 600 mL of deionized water to form a slurry. The slurry was allowed to settle before decanting, a process repeated three times to eliminate impurities. Following the final decantation, the upper layer was removed, and the remaining slurry was sieved and dried at approximately 100°C for 24 hours. The dried material was then finely ground and sieved to obtain particles with a size of less than 100 µm. The refined kaolin, along with the heavier fractions from the settling process, was analyzed using X-ray fluorescence (XRF), X-ray diffraction (XRD), Fourier transform infrared spectroscopy (FTIR), and scanning electron microscopy (SEM) to determine its composition and structural properties.

Fig. 2. A picture of the kaolin from Ajebo in Ogun State, Nigeria

2.2 Dealumination of kaolin and metakaolinization

The washed and dried 100 µm kaolin underwent a leaching process to reduce the Al_2O_3 present in the kaolinite structure. Acid leaching was carried out using hydrochloric acid (HCl) with a molar concentration of 32 M and 99 wt. %. The refined kaolin was poured into a container, and then HCl and distilled water were added at a percentage rate of 15% and 85%, respectively. The mixture was allowed to settle for 30 minutes and then decanted. The top layer was decanted, and 3.5 litres of distilled water were added to the base layer for washing. The addition of distilled water and decantation were repeated consecutively until the acid was thoroughly washed from the kaolin, which was then ready for further leaching with sulphuric acid. The kaolin sample underwent further leaching by adding distilled water and H_2SO_4 with a molar concentration of 18.76 M and 98 wt. %. After settling for 24 hours, the mixture formed two layers; the top layer was decanted, and 1 litre of hydrochloric acid with the same concentration as the first leaching was added to the base layer, allowing for proper penetration into the solution. The resulting solution was kept in an oven at 80 ºC for 30 minutes. The top layer was decanted, leaving the base layer behind. About 3.5 litres of distilled water were then added to the base layer (leached kaolin sample) and allowed to settle for 30 minutes to remove any acid present in the base layer. After settling, the distilled water was decanted. This process was

repeated three times, and after each decantation, a leached kaolin solution with fewer impurities remained. The resulting kaolin sample was left behind, which was thoroughly leached. This kaolin was further subjected to heat for proper drying, and the output result is shown in Fig. 3. The metakaolinization process involved heating the acid-leached kaolin samples in a muffle furnace at 900°C for 2 hours.

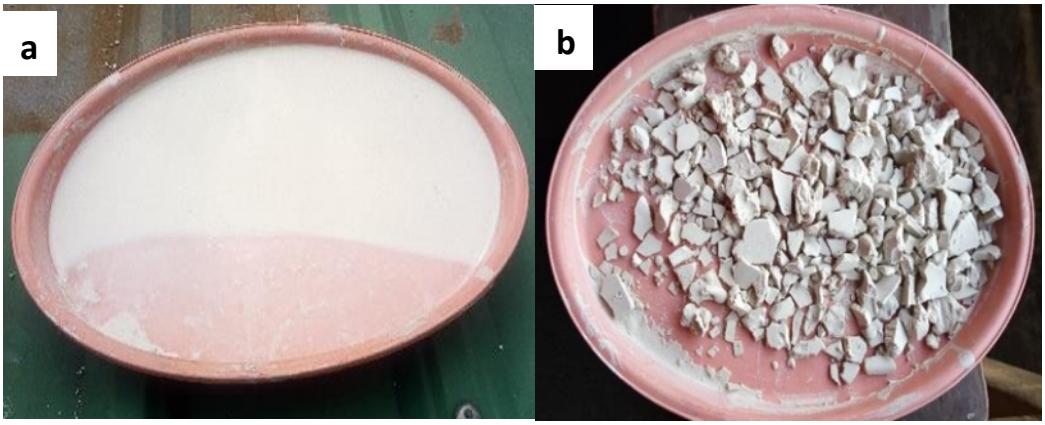

Fig. 3. Leached kaolin in liquid and dried Form

2.3 Hydrothermal synthesis of ZSM-5 from refined kaolin samples

The hydrothermal synthesis process of ZSM-5 conducted in this study followed the procedure described in [3,13,16]. A schematic representation of the synthesis process is shown in Fig. 4. The procedure commenced with the preparation of a sodium hydroxide (NaOH) solution by dissolving 2.3 grams of NaOH pellets in 166 mL of distilled water. Following this, 2.0 grams of metakaolin were introduced into the solution and stirred vigorously for 5 minutes. Subsequently, 15 grams of external silica (sodium silicate) were added to the mixture to form a gel, which was continuously stirred for approximately 2 hours to achieve uniformity.

Once a homogeneous gel was obtained, it was aged for 24 hours. Three separate samples were prepared using the same gel composition and ageing conditions. These samples were then subjected to hydrothermal treatment at varying crystallization temperatures of 100°C, 120°C, and 150°C. The crystallization process took place in an oven for 6 hours. Upon completion, the reactions were halted, and the samples were allowed to cool to room temperature.

After cooling, the samples were thoroughly washed and subsequently dried at 150°C. The final products were analyzed using X-ray fluorescence (XRF), X-ray diffraction (XRD), scanning electron microscopy (SEM), and Fourier transform infrared spectroscopy (FTIR) to assess their structural and compositional properties.

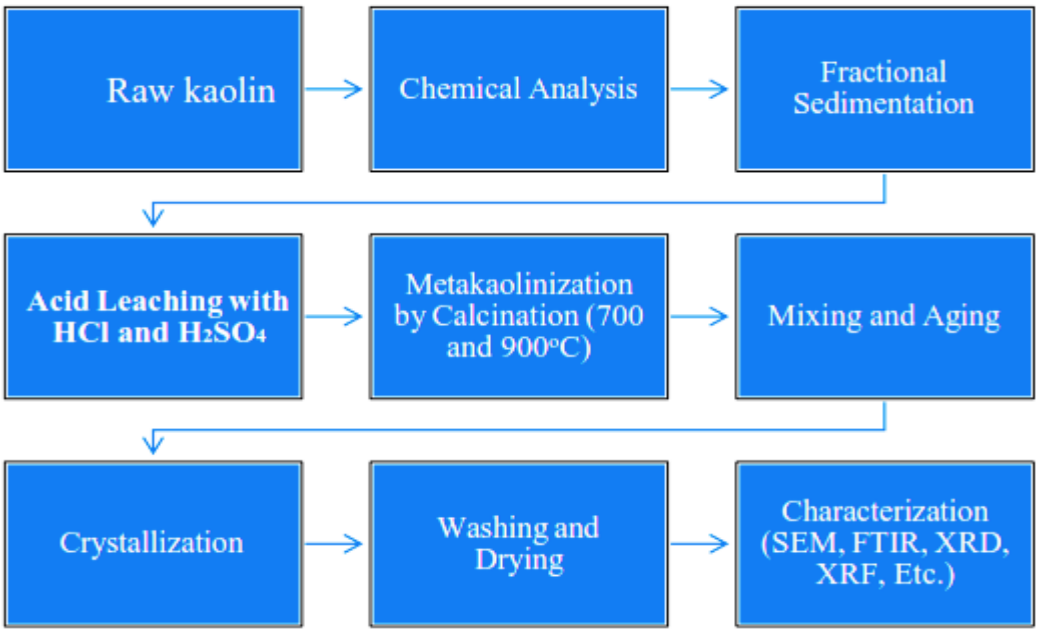

Fig. 4. Schematic representation of the synthesis process of ZSM-5

2.4 Sample Characterization

Various analytical characterization techniques were employed to examine the raw kaolin, metakaolin, and synthesized zeolite products across different crystallization temperatures. The chemical composition of the samples was analyzed using an X-ray fluorescence (XRF) spectrometer (model XL 3t-950, Thermo Scientific Niton). The results were presented in both elemental and oxide forms, identifying the primary elements present.

X-ray diffraction (XRD) analysis was performed to examine the crystalline structures of the kaolinite and synthesized zeolite using a Bruker D8 Discover diffractometer (Bruker AXS, Karlsruhe, Germany). This instrument featured a Cu$K\alpha$ radiation source (λ = 1.54056 Å) and operated at 50 kV and 1000 µA. XRD patterns were recorded within a 2θ range of 10° to 80°, with a step size of 8.75° and a scan duration of 400 seconds per step.

Fourier-transform infrared spectroscopy (FTIR) was employed to identify functional groups in the kaolinite and zeolite samples. A Shimadzu IR Affinity-1S spectrometer (Shimadzu Corporation, Japan) was used for the analysis. Each sample (0.01 g) was finely ground with an equal amount of KBr using an agate mortar and pestle before measurement. The spectra were recorded in the wavelength range of 400 to 4000 cm^{-1}.

Scanning electron microscopy (SEM) was utilized to investigate the surface morphology and elemental distribution of the samples. The analysis was conducted using an ASPEX 3020 SEM (Aspex Corporation) equipped with energy-dispersive X-ray spectroscopy (EDX). Before imaging, the samples were coated to enhance conductivity. High-resolution SEM imaging was performed at an accelerating voltage of 5.00 kV.

3. Results and Discussion

3.1 Chemical Analysis

The chemical composition of Ajebo Kaolin and its refined forms (metakaolin and synthesized zeolite products) are summarized in Table 1. The primary constituents of kaolin, silica (SiO_2), and

alumina (Al_2O_3) were found to be present in the Ajebo Kaolin at 42.15 wt.% and 28.5 wt.%, respectively. The calculated SiO_2/Al_2O_3 ratio of 1.478 is close to the theoretical value of 1 for pure kaolinite, suggesting that the kaolin is suitable for direct use in zeolite synthesis [1]. The transformation of Ajebo Kaolin into metakaolin increased the SiO_2/Al_2O_3 ratios, accompanied by a decrease in the weight percentage of oxides, as shown in Table 1. This indicates that the leaching process effectively removed impurities from the raw kaolin. According to literature reports [11,38,39] the SiO_2/Al_2O_3 ratio of 1 is achievable only in pure kaolin containing 100% kaolinite. However, during treatment processes like leaching or calcination, this ratio may deviate due to alterations in chemical constituents caused by the process and the reagents used. Mineralogical analysis of the kaolin via XRF revealed the presence of kaolinite ($Al_2Si_2O_5(OH)_4$), muscovite ($KAl_2(Si_3Al)O_{10}(OH, F)_2$), and quartz ($SiO_2$). The quartz content is attributed to the high SiO_2 levels found in the raw kaolin, consistent with findings from other geological kaolin studies [1]. The chemical composition of the synthesized zeolite samples and those crystallized at different temperatures is also presented in Table 1. SiO_2 and Al_2O_3 remain the primary constituents of ZSM-5 across all the studied crystallization temperatures. It was observed that the alumina content in the kaolin decreased following thermal treatment, resulting in Si/Al ratios of 2.54, 2.47, and 2.44, respectively. This reduction is attributed to the bonding of some surface Al ions in the zeolite with silicate ions. Additionally, sulfur was absent in the as-synthesized zeolite but appeared in the modified zeolite, introduced during the modification process with H_2SO_4. This confirms the successful chemical modification of the zeolite, aligning with findings on surface modification of zeolites reported in the literature [11].

Table 1
Chemical composition of the raw kaolin, metakaolin, and zeolites

	Oxides composition (wt. %)									
	SiO_2	**Al_2O_3**	**Na_2O**	**TiO_2**	**Fe_2O_3**	**P_2O_5**	**Na_2O**	**K_2O**	**CaO**	**L.O.I**
Ajebo Kaolin	42.15	28.5	1.5969	0.96	1.78	0.027	0.98	0.1339	0.1241	12.8275
Metakaolin	28.89	16.6	0.3253	0.15	1.52	0.003	0.12	0.1048	0.2877	0.1452
ZSM-5/100°C	43.69	17.2	0.5857	0. 6	1.12	0.01	0.22	0.2002	0.0364	3.5225
ZSM-5/120°C	44.39	17.96	0.5752	0.06	1.58	0..017	0.32	0.2033	0.3516	1.6744
ZSM-5/150°C	44.80	18.38	0.66	0.013	1.98	0.031	0.24	0.18	0.58	0.9

3.2 X-ray diffraction (XRD) analysis

Fig. 5 illustrates the XRD patterns of Ajebo kaolin and calcined (metakaolin) kaolin samples. The Ajebo kaolin sample is characterized by distinct kaolinite X-ray diffraction peaks at 2θ = 12.4° and 24.88°, aligning with previous reports [3, 6, 7, 12]. The X-ray diffraction (XRD) patterns of metakaolin samples, calcined at 900°C for 2 hours, are presented in Fig. 5b. A significant transformation is apparent when compared to the XRD pattern of the uncalcined sample. The calcined samples show reduced peak intensities, and the characteristic kaolinite peaks are absent. This suggests a structural change, where kaolin transitions from a crystalline phase to an amorphous phase during the metakaolinization process. The broad nature of the diffraction peaks indicates the formation of an

amorphous structure, while the presence of crystalline silica in the clay contributes to the residual peaks even after calcination.

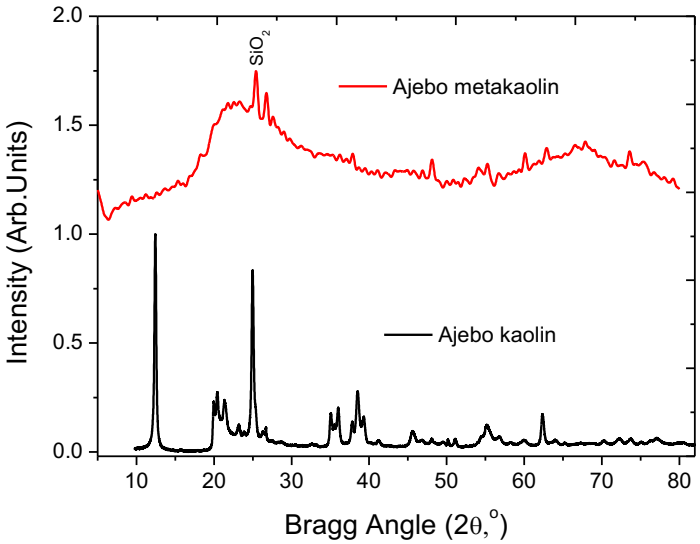

Fig. 5. XRD pattern of (a) Ajebo kaolin and (b) Ajebo metakaolin

The XRD patterns of the Ajebo kaolin-based ZSM-5 zeolite synthesized at crystallization temperatures of 100°C, 120°C, and 150°C are presented in Fig. 6 (a-c). These patterns reveal the presence of ZSM-5 zeolite, with characteristic peaks observed at 2θ values of 31–40°, 41°, 42°, 63–64°, 71°, 72°, and 77–78°. These weaker peaks somehow confirm the formation of ZSM-5 crystals but with significant impurities in the synthesized products. However, variations in peak intensity are observed across different crystallization temperatures, highlighting the significant role temperature plays in the zeolite synthesis process. The XRD pattern at 100°C (Fig. 6a) shows strong peaks at 2θ = 31–40° and weak peaks at 77–78°, indicating the formation of ZSM-5 crystals, albeit with limited crystallinity. At 120°C (Fig. 6b), a prominent amorphous peak appears, indicating the presence of amorphous aluminosilicate. As the nucleation rate increases with rising temperature, the amorphous gel transitions into a pure, crystalline ZSM-5 phase [1, 32]. The XRD pattern at 150°C (Fig. 6c) demonstrates significant improvements in crystallinity. Strong peaks at 2θ = 31–40°, 41°, and 42°, along with weaker peaks at 72° and 77–78°, confirm the presence of ZSM-5 with enhanced crystal growth. These results highlight the significant impact of temperature on nucleation and crystal growth during zeolite synthesis, as higher temperatures facilitate the formation of a well-defined crystalline structure [11,33]. The observed XRD peaks generally suggest the presence of unreacted quartz (SiO_2) and other residual clay minerals, rather than pure ZSM-5 zeolite. Typical ZSM-5 zeolite, which belongs to the MFI (Mobil Five) framework, exhibits its most characteristic peaks in the 5°–10° and 22°–25° regions, with weaker peaks appearing between 45° and 50°**.** The absence of these key ZSM-5 peaks and the dominance of higher-angle reflections indicate incomplete crystallization, the persistence of parent clay phases, or the formation of secondary aluminosilicate phases such as mullite or feldspar**.** This suggests that the hydrothermal synthesis process did not fully transform the clay into pure ZSM-5, possibly due to inadequate reaction time and temperature, insufficient templating agent, or suboptimal synthesis conditions, which necessitated further analysis, such as SEM-EDX and FTIR measurements, to confirm the extent of ZSM-5 formation and to optimize the crystallization process.

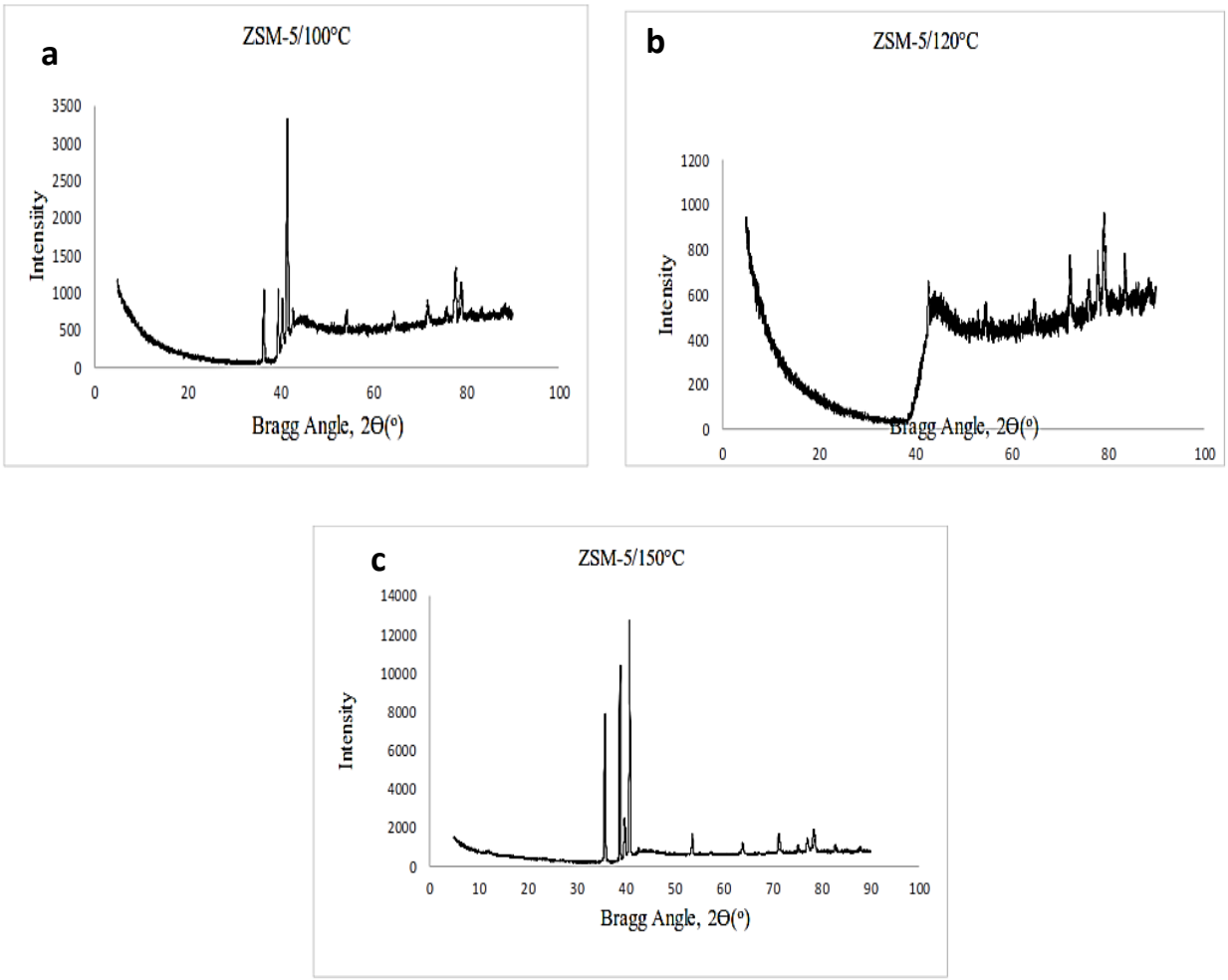

Fig. 6. XRD Pattern of (a) ZSM-5/100°C (b) ZSM-5/120°C (c) ZSM-5/150°C

3.3 Spectral Analysis using FTIR

The FTIR spectra of kaolin and metakaolin are presented in Fig. 7. The FTIR spectrum identifies the absorption bands and their relation to the vibration modes of chemical bonds on the sample surface. The FTIR spectrum of kaolin confirms the presence of -OH stretching and bending vibrations between 3600 and 3700 cm^{-1}, characteristic of kaolinite. The absence of the -OH stretching bands in the metakaolin spectrum verifies the successful dehydroxylation and transition from kaolin to metakaolin. This transformation is further supported by the broad peaks in the XRD patterns, indicating the structural shift from crystalline kaolin to amorphous metakaolin. In the FTIR spectrum of kaolinite, the -OH stretching and bending bands provide valuable insights into the structural order within the kaolin framework. According to Vaculíková et al. [40] , kaolinite can be categorized into three structural order types based on the positioning and relative intensity of the -OH bands. The Ajebo kaolin used in this study exhibits a highly ordered structure, as evidenced by the well-defined -OH stretching and bending bands characterized by four distinct stretching peaks between 3600 and 3700 cm^{-1}, with notable signals at 3620.51 and 3695.73 cm^{-1}, along with two weaker peaks in the same range. The lack of signals within the 3600–3700 cm^{-1} range indicates the loss of hydroxyl groups, confirming the dehydroxylation process and the conversion of kaolin to metakaolin. Structural changes due to heating are also apparent, such as modifications in the Si-O bonding plane

stretch at 1077 cm^{-1}, resulting from valence vibrations. Additionally, the translation of the hydroxyl group within the kaolin lattice is characterized by a wavenumber near 796 cm^{-1} [13].

Figure 8 displays the FTIR spectra of the synthesized ZSM-5 samples, emphasizing signals related to molecular structures, functional groups, and organic bonds. The broad peaks observed at 3486 and 3785 cm^{-1} correspond to zeolitic -OH functional groups. Key bands include 795 cm^{-1} due to external symmetric stretching vibration, 1050–1150 cm^{-1} corresponding to internal asymmetric stretching vibrations, and 1224 cm^{-1} as a result of external asymmetric stretching vibration [34,37]. The absorption bands in the range of 3471–3655 cm^{-1} are associated with the stretching vibrations of terminal Si-OH groups and adsorbed water molecules, while bands between 1631 and 1650 cm^{-1} relate to the vibrations of -OH groups. The characteristic vibrations of the zeolite framework, especially the asymmetric and symmetric stretching of T-O-T (where T represents Si and Al) groups, correspond to bands observed within 1085–1100 cm^{-1} and 798–810 cm^{-1}. Compared to ZSM-5 zeolites reports in the literature, not all the peaks in this study were formed entirely. This is possibly due to incomplete crystallization resulting from the limited 6-hour crystallization time.

The influence of temperature on the ZSM-5 zeolite structure is reflected in the spectral variations. As the temperature increases from 100°C to 150°C, the wavenumber at 500 cm^{-1}, which corresponds to the intense four-membered rings of the pentasil structure, becomes more pronounced, indicating an enhanced crystallinity of the ZSM-5 zeolite. Additionally, the peak at 962 cm^{-1}, representing asymmetric vibrations from overlapping Si-O bridging and Si-O non-bridging bonds, further confirms the structural integrity of the synthesized ZSM-5 zeolite.

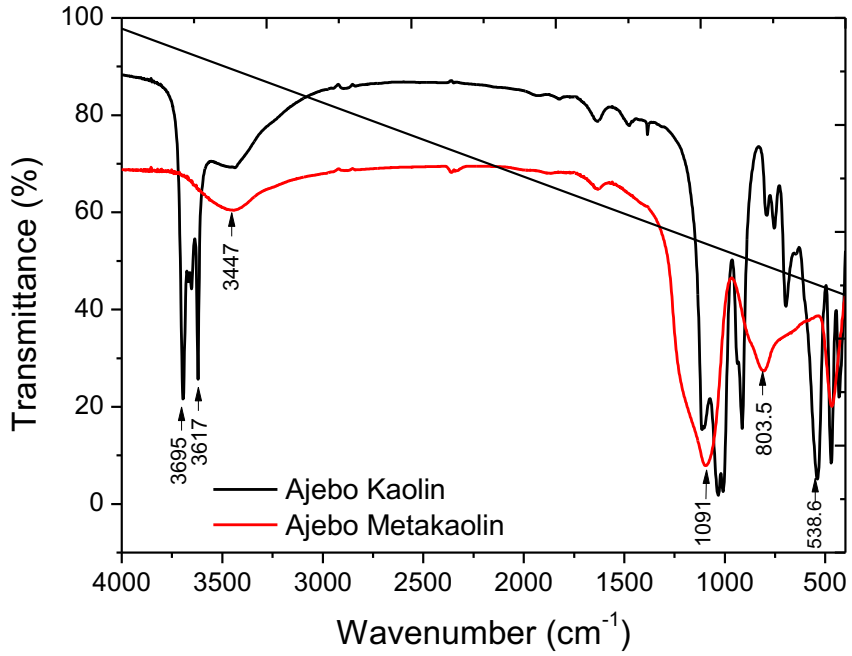

Fig. 7. FTIR spectra of (a) Ajebo Kaolin (b) Metakaolin

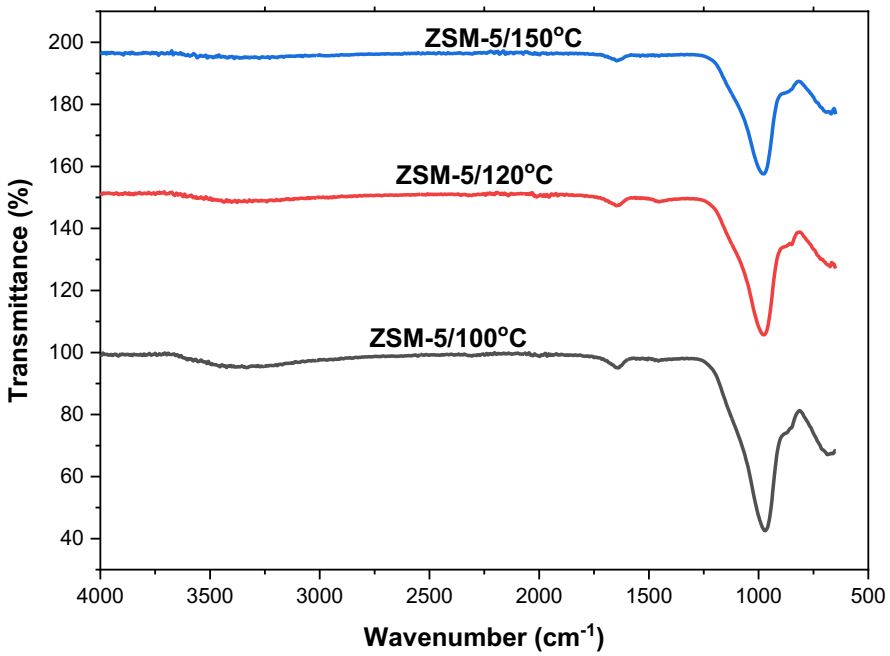

Fig. 8. FTIR spectra of synthesized zeolite showing the effect of crystallization temperature

3.3 Morphological analysis using SEM

Fig. 9 displays the SEM images of kaolin and metakaolin, highlighting the morphological changes that occur during the transformation of kaolin into metakaolin. The raw Ajebo kaolin (Fig. 9a) exhibits a plate-like structure, characteristic of kaolinite materials. This structure indicates the ordered and crystalline nature of the raw kaolin. In contrast, metakaolin (Fig. 9b) shows a distinct lump-like structure, a direct consequence of its highly amorphous nature, as noted in previous studies [10,22]. This transformation into an amorphous phase occurs due to the dehydroxylation and structural changes that happen during the calcination process.

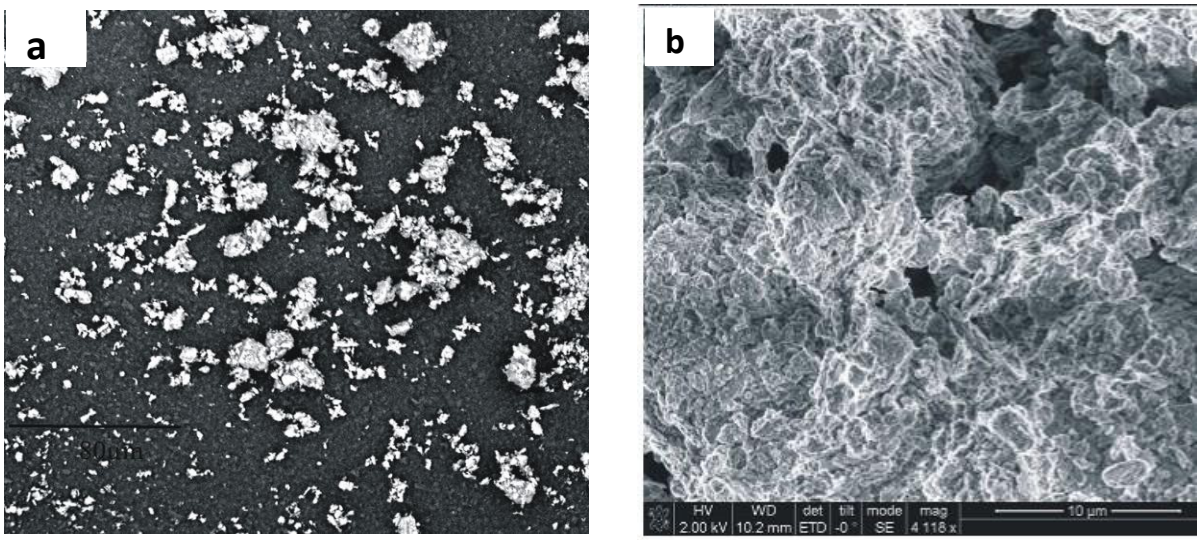

Fig. 9. SEM images of (a) Ajebo Kaolin (b) Metakaolin

The morphology of metakaolinite is crucial in synthesizing zeolites, as the characteristics of the starting material can significantly influence the final product. For example, incomplete metakaolinization or the use of untreated kaolin may lead to the formation of sodalite instead of zeolite-A [1,41]. Furthermore, the SEM images of Ajebo kaolin show large aggregates of disordered stacks of platelets, which can affect the reactivity of the kaolin during the synthesis process, thereby impacting the efficiency and quality of the final zeolite product [42,43].

The SEM analysis of the synthesized ZSM-5 zeolite at various crystallization temperatures (Fig. 10a–c), in conjunction with energy-dispersive X-ray (EDX) spectroscopy, provides critical insights into the evolution of morphological features, crystallization behavior, and phase composition. The transformation of the irregular lamellar kaolinite precursor into highly crystalline ZSM-5 zeolite with distinct morphologies is evident across different temperatures. Hydrothermal and solid-state thermal treatments facilitated the development of well-defined hexagonal prismatic crystals, with particle sizes ranging between 400 and 600 nm—consistent with the characteristic morphology of ZSM-5 zeolite [30,31,43]. The degree of crystal growth, agglomeration, and structural integrity was influenced by the kaolin source and synthesis parameters [1,42]. At 100°C (Fig. 10a), the sample exhibited predominantly amorphous structures with only a few scattered hexagonal particles, indicating the early stage of ZSM-5 crystallization. The limited nucleation and crystal growth at this stage suggest incomplete conversion of the aluminosilicate precursor. As the temperature increased to 120°C (Fig. 10b), a notable enhancement in crystallinity and particle intergrowth was observed, with the formation of moderately aggregated prismatic ZSM-5 crystals. At 150°C (Fig. 10c), the synthesized zeolite displayed well-formed hexagonal prisms with higher crystallinity and increased intergrowth, demonstrating the temperature-dependent evolution of metastable zeolite phases [23,37]. This progression underscores the crucial role of thermal energy in promoting phase transitions, nucleation kinetics, and optimized crystal formation. The EDX spectra further confirmed the presence of sodium, originating from NaOH used in the synthesis process. Sodium plays a vital role in templating and stabilizing the zeolite framework, acting as an equilibrium cation during crystallization. The measured Si/Al atomic ratio of 1.38 aligns with X-ray fluorescence (XRF) results, indicating an optimal balance between silica and alumina content, which directly influences the catalytic and adsorption properties of the synthesized ZSM-5 zeolite [10]. These findings collectively validate the successful transformation of kaolinite into ZSM-5 and emphasize the significance of controlled crystallization temperature in tailoring zeolite morphology and phase composition.

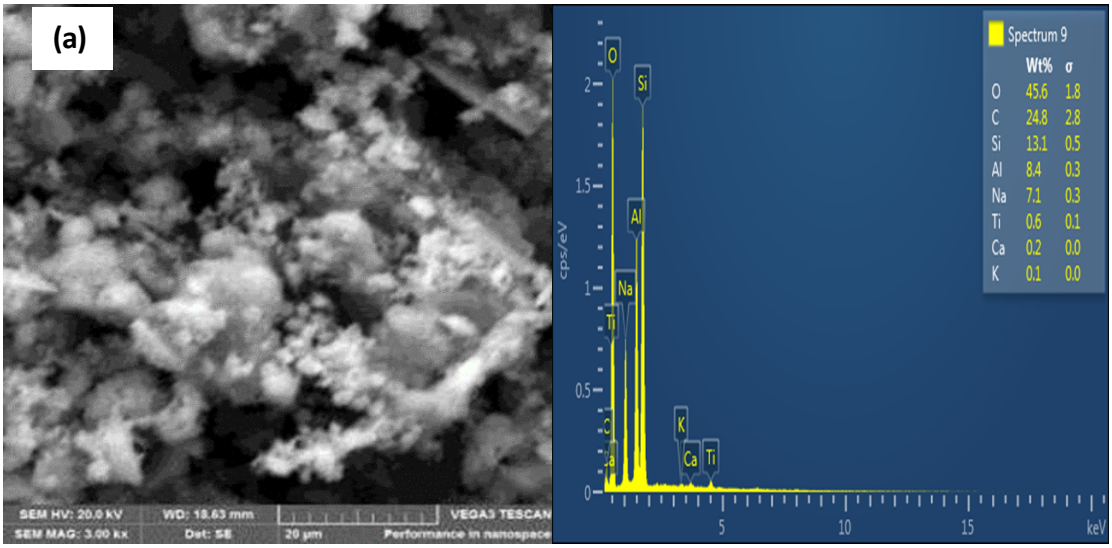

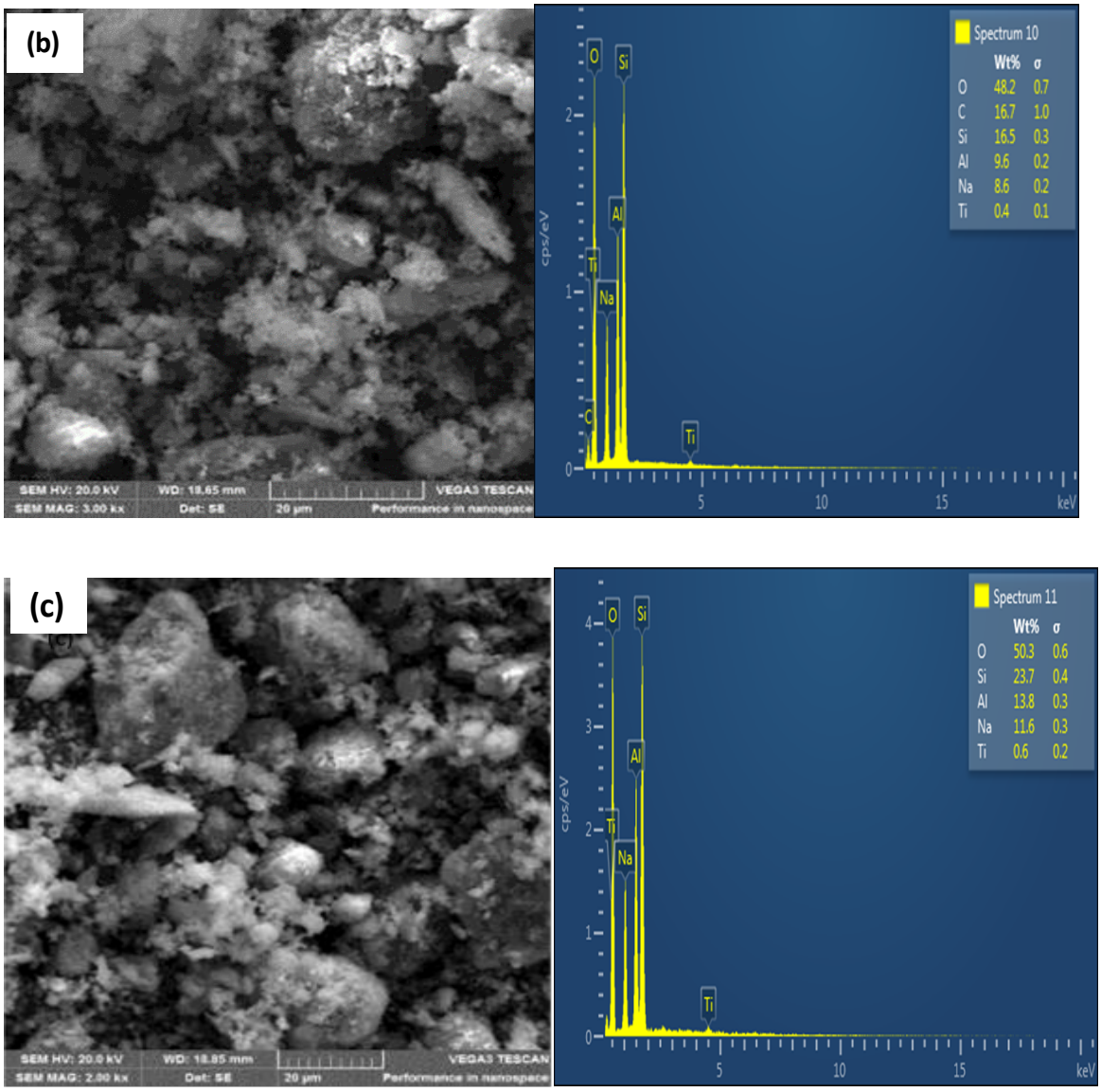

Fig. 10. SEM/EDS of (a) ZSM-5/100°C (b) ZSM-5/120°C (c) ZSM-5/150°C

4. Conclusion

ZSM-5 zeolite was successfully synthesized from Ajebo kaolin, with the effects of crystallization temperature and morphology on its formation extensively explored. The results underscore the critical role of temperature and reaction time in achieving high crystallinity and well-defined ZSM-5 structures. While characterization through XRD, FTIR, XRF, EDX, and SEM confirmed the formation of ZSM-5, the XRD patterns also indicated the presence of residual amorphous phases and unreacted silica, suggesting incomplete transformation under certain conditions. XRF analysis confirmed that silica and alumina were the dominant components, validating Ajebo kaolin as a viable raw material. FTIR spectra revealed the successful dehydroxylation of kaolinite, evidenced by the disappearance of -OH stretching and bending bands (3600–3700 cm^{-1}) in metakaolin. The transformation of kaolin from a crystalline to an amorphous phase during metakaolinization was also confirmed via XRD, which is crucial for zeolite formation. The synthesized ZSM-5 zeolite exhibited a distinct FTIR peak near 1078 cm^{-1}, a signature of its MFI framework, while EDX detected sodium, originating from the use of NaOH as a mineralizing agent. SEM micrographs showed improved hexagonal prismatic

structures in the sample synthesized at 150°C, demonstrating well-developed ZSM-5 morphology. However, the presence of high-angle XRD reflections (31°–78°) suggested the retention of some quartz and secondary aluminosilicate phases, which could impact catalytic performance. Among the samples, the one synthesized at 150°C exhibited the highest crystallinity, confirming the influence of temperature in optimizing zeolite properties. This study highlights the potential of Nigeria's Ajebo kaolin as a cost-effective and sustainable source of alumina and silica for ZSM-5 synthesis. The resulting ZSM-5 zeolite shows strong potential for catalytic applications, particularly in hydrocarbon degradation, paving the way for its utilization in industrial refining and petrochemical processes.

Statements and Declarations

Competing interest: The authors declare that they have no known financial or competing interests that could have appeared to influence the work reported in this paper.

Funding: The authors did not receive support from any organization for the submitted work.

Availability of data and material: The necessary data used in the manuscript is already present.

Authors' contributions: Conceptualization: [Henry E. Mgbemere, Augustine B. Okoubulu]; Methodology: [Augustine B. Okoubulu, Henry E. Mgbemere]; Formal analysis and investigation: [Augustine B. Okoubulu, Henry E. Mgbemere, Cynthia C. Nwaeju]; Writing - original draft: [Henry E. Mgbemere, Augustine B. Okoubulu, Cynthia C. Nwaeju, Francis O. Edoziuno]; Writing - review and editing: [Cynthia C. Nwaeju, Francis O. Edoziuno, Pius A. Uzere, Augustine B. Okoubulu]; Supervision: [Henry E. Mgbemere].

References

[1] Mohiuddin, E., Y. M. Isa, M. M. Mdleleni, N. Sincadu, D. Key, and T. Tshabalala. "Synthesis of ZSM-5 from Impure and Beneficiated Grahamstown Kaolin: Effect of Kaolinite Content, Crystallisation Temperatures and Time." *Applied Clay Science* 119 (2016): 213–221. https://doi.org/10.1016/j.clay.2015.10.008.

[2] Maciver, V. P., K. K. Dagde, and J. L. Konne. "Synthesis of Zeolite X from Locally Sourced Kaolin Clay from Kono-Boue and Chokocho, Rivers State, Nigeria." *Advances in Chemical Engineering and Science* 10 (2020): 399–407. https://doi.org/10.4236/aces.2020.104025.

[3] Aliyu, U. M., S. Rathilal, S. I. Mustapha, R. Musamali, and E. K. Tetteh. "Hydrothermal Synthesis of Kaolin-Based ZSM-5 Zeolite: Effect of Synthesis Parameters and Its Application for Bioethanol Conversion." *Catalysis Communications* 182 (2023): 106750. https://doi.org/10.1016/j.catcom.2023.106750.

[4] Far, R. M., B. Van der Bruggen, A. Verliefde, and E. Cornelissen. "A Review of Zeolite Materials Used in Membranes for Water Purification: History, Applications, Challenges and Future Trends." *Journal of Chemical Technology and Biotechnology* 97 (2022): 575–596. https://doi.org/10.1002/jctb.6963.

[5] Ren, W., J. Li, L. Han, B. Wang, J. Wang, L. Chang, and W. Bao. "One-Step Synthesis of Zeolite ZSM-5 from Perlite Tailings by Crystal Seed Solution Assisted Method." *Fuel* 374 (2024): 132489. https://doi.org/10.1016/j.fuel.2024.132489.

[6] Gao, S., H. Peng, B. Song, J. Zhang, W. Wu, J. Vaughan, P. Zardo, J. Vogrin, S. Tulloch, and Z. Zhu. "Synthesis of Zeolites from Low-Cost Feeds and Its Sustainable Environmental Applications." *Journal of Environmental Chemical Engineering* 11 (2023): 108995. https://doi.org/10.1016/j.jece.2022.108995.

[7] Han, C., J. Yang, S. Dong, L. Ma, Q. Dai, and J. Guo. "Zeolite Preparation from Industrial Solid Waste: Current Status, Applications, and Prospects." *Separation and Purification Technology* 354 (2025): 128957. https://doi.org/10.1016/j.seppur.2024.128957.

[8] Lafi, A. A. F., S. K. Matam, and H. A. Hodali. "New Synthesis of ZSM-5 from High-Silica Kaolinite and Its Use in Vapor-Phase Conversion of 1-Phenylethanol to Styrene." *Industrial & Engineering Chemistry Research* 54 (2015): 3754–3760.

[9] Akoji, J. N., and W. Mohammed. "Nano Trends: Synthesis and Application of Zeolite A from Kaolin Obtained from Dei Dei, Bwari Area Council, Abuja." 34–42, 2023. https://doi.org/10.37591/NTs.

[10] Kovo, A. S., O. Hernandez, and S. M. Holmes. "Synthesis and Characterization of Zeolite Y and ZSM-5 from Nigerian Ahoko Kaolin Using a Novel, Lower Temperature, Metakaolinization Technique." *Journal of Materials Chemistry* 19 (2009): 6207. https://doi.org/10.1039/b907554b.

[11] Tabi, R. N., F. O. Agyemang, K. Mensah-Darkwa, E. K. Arthur, E. Gikunoo, and F. Momade. "Zeolite Synthesis and Its Application in Water Defluorination." *Materials Chemistry and Physics* 261 (2021): 124229. https://doi.org/10.1016/j.matchemphys.2021.124229.

[12] Zdretsov, I. M., and A. M. Gerasimov. "Green and Low-Cost Synthesis of Zeolites from Kaolin: A Promising Technology or a Delusion?" *Reaction Chemistry & Engineering* 9 (2024): 1994–2027.

[13] Mgbemere, H. E., G. I. Lawal, and I. C. Ekpe. "Synthesis of Zeolite-A Using Kaolin Samples from Darazo, Bauchi State and Ajebo, Ogun State in Nigeria." *Nigerian Journal of Technology* 37 (2018): 87–95.

[14] Mohiuddin, E., Y. M. Isa, M. M. Mdleleni, and D. Key. "Effect of Kaolin Chemical Reactivity on the Formation of ZSM-5 and Its Physicochemical Properties." *Microporous and Mesoporous Materials* 237 (2017): 1–11. https://doi.org/10.1016/j.micromeso.2016.08.028.

[15] Ayele, L., J. Pérez-Pariente, Y. Chebude, and I. Díaz. "Synthesis of Zeolite A from Ethiopian Kaolin." *Microporous and Mesoporous Materials* 215 (2015): 29–36. https://doi.org/10.1016/j.micromeso.2015.05.022.

[16] Wang, J.-Q., Y.-X. Huang, Y. Pan, and J.-X. Mi. "Hydrothermal Synthesis of High Purity Zeolite A from Natural Kaolin without Calcination." *Microporous and Mesoporous Materials* 199 (2014): 50–56. https://doi.org/10.1016/j.micromeso.2014.08.002.

[17] Panpa, W., and S. Jinawath. "Synthesis of ZSM-5 Zeolite and Silicalite from Rice Husk Ash." *Applied Catalysis B: Environmental* 90 (2009): 389–394. https://doi.org/10.1016/j.apcatb.2009.03.029.

[18] Jiang, N., R. Shang, S. G. J. Heijman, and L. C. Rietveld. "High-Silica Zeolites for Adsorption of Organic Micro-Pollutants in Water Treatment: A Review." *Water Research* 144 (2018): 145–161. https://doi.org/10.1016/j.watres.2018.07.017.

[19] Chareonpanich, M., O. Jullaphan, and C. Tang. "Bench-Scale Synthesis of Zeolite A from Subbituminous Coal Ashes with High Crystalline Silica Content." *Journal of Cleaner Production* 19 (2011): 58–63. https://doi.org/10.1016/j.jclepro.2010.08.012.

[20] Argauer, R. J., and G. R. Landolt. "Crystalline Zeolite ZSM-5 and the Method of Preparing the Same." Patent, 1972.

[21] Gougazeh, M., and J.-C. Buhl. "Synthesis and Characterization of Zeolite A by Hydrothermal Transformation of Natural Jordanian Kaolin." *Journal of the Association of Arab Universities for Basic and Applied Sciences* 15 (2014): 35–42. https://doi.org/10.1016/j.jaubas.2013.03.007.

[22] Ren, Z., L. Wang, Y. Li, J. Zha, G. Tian, F. Wang, H. Zhang, and J. Liang. "Synthesis of Zeolites by In-Situ Conversion of Geopolymers and Their Performance of Heavy Metal Ion Removal in Wastewater: A Review." *Journal of Cleaner Production* 349 (2022): 131441.

[23] Chareonpanich, M., T. Namto, P. Kongkachuichay, and J. Limtrakul. "Synthesis of ZSM-5 Zeolite from Lignite Fly Ash and Rice Husk Ash." *Fuel Processing Technology* 85 (2004): 1623–1634. https://doi.org/10.1016/j.fuproc.2003.10.026.

[24] Murray, H. H. "Traditional and New Applications for Kaolin, Smectite, and Palygorskite: A General Overview." *Applied Clay Science* 17 (2000): 207–221. https://doi.org/10.1016/S0169-1317(00)00016-8.

[25] Bergaya, F., and G. Lagaly. "Chapter 1: General Introduction: Clays, Clay Minerals, and Clay Science." In *Handbook of Clay Science*, edited by F. Bergaya and G. Lagaly, 1–18. Amsterdam: Elsevier, 2006. https://doi.org/10.1016/S1572-4352(05)01001-9.

[26] Alaba, P. A., Y. M. Sani, and W. M. A. W. Daud. "Kaolinite Properties and Advances for Solid Acid and Basic Catalyst Synthesis." *RSC Advances* 5 (2015): 101127–101147. https://doi.org/10.1039/C5RA18884A.

[27] Ghrib, Y., N. Frini-Srasra, E. Srasra, J. Martínez-Triguero, and A. Corma. "Synthesis of Co-Crystallized USY/ZSM-5 Zeolites from Kaolin and Its Use as Fluid Catalytic Cracking Catalysts." *Catalysis Science & Technology* 8 (2018): 716–725. https://doi.org/10.1039/C7CY01477E.

[28] Abdullahi, T., Z. Harun, and M. H. D. Othman. "A Review on Sustainable Synthesis of Zeolite from Kaolinite Resources via Hydrothermal Process." *Advanced Powder Technology* 28 (2017): 1827–1840. https://doi.org/10.1016/j.apt.2017.04.028.

[29] Collins, F., A. Rozhkovskaya, J. G. Outram, and G. J. Millar. "A Critical Review of Waste Resources, Synthesis, and Applications for Zeolite LTA." *Microporous and Mesoporous Materials* 291 (2020): 109667. https://doi.org/10.1016/j.micromeso.2019.109667.

[30] Chandrasekhar, S. "Influence of Metakaolinization Temperature on the Formation of Zeolite 4A from Kaolin." *Clay Minerals* 31 (1996): 253–261. https://doi.org/10.1180/claymin.1996.031.2.11.

[31] Wu, G., W. Wu, X. Wang, W. Zan, W. Wang, and C. Li. "Nanosized ZSM-5 Zeolites: Seed-Induced Synthesis and the Relation between the Physicochemical Properties and the Catalytic Performance in the Alkylation of

Naphthalene." *Microporous and Mesoporous Materials* 180 (2013): 187–195. https://doi.org/10.1016/j.micromeso.2012.11.011.

[32] Aguilar-Mamani, W., G. García, J. Hedlund, and J. Mouzon. "Comparison between Leached Metakaolin and Leached Diatomaceous Earth as Raw Materials for the Synthesis of ZSM-5." *SpringerPlus* 3 (2014): 292.

[33] Hartati, H., A. A. Widati, T. K. Dewi, and D. Prasetyoko. "Direct Synthesis of Highly Crystalline ZSM-5 from Indonesian Kaolin." *Bulletin of Chemical Reaction Engineering & Catalysis* 12 (2017): 251–255.

[34] Hartanto, D., R. Kurniawati, A. B. Pambudi, W. P. Utomo, W. L. Leaw, and H. Nur. "One-Pot Non-Template Synthesis of Hierarchical ZSM-5 from Kaolin Source." *Solid State Sciences* 87 (2019): 150–154.

[35] Hartanto, D., A. B. Pambudi, D. N. Cahyanti, and W. P. Utomo. "On the Synthesis of ZSM-5 Directly from Kaolin Bangka with Aging Time." In *Indonesia Malaysia Research Consortium Seminar 2018 (IMRCS 2018)*, 012039. 2018.

[36] artanto, D., L. S. Yuan, S. M. Sari, D. Sugiarso, I. K. Murwani, T. Ersam, D. Prasetyoko, and H. Nur. "Can Kaolin Function as Source of Alumina in the Synthesis of ZSM-5 without an Organic Template Using a Seeding Technique?" *Malaysian Journal of Fundamental and Applied Sciences* 12 (2016): 85–90.

[37] Khatamian, M., and M. Irani. "Preparation and Characterization of Nanosized ZSM-5 Zeolite Using Kaolin and Investigation of Kaolin Content, Crystallization Time and Temperature Changes on the Size and Crystallinity of Products." *Journal of the Iranian Chemical Society* 6 (2009): 187–194. https://doi.org/10.1007/BF03246519.

[38] Jamo, H. U. "Structural Analysis and Surface Morphology of Quartz." *Bayero Journal of Pure and Applied Sciences* 9 (2017): 230. https://doi.org/10.4314/bajopas.v9i2.40.

[39] Yahaya, S., S. S. Jikan, N. A. Badarulzaman, and A. D. Adamu. "Chemical Composition and Particle Size Analysis of Kaolin." *Path of Science* 3 (2017): 1001–1004. https://doi.org/10.22178/pos.27-1.

[40] Vaculikova, L., E. Plevova, S. Vallova, and I. Koutnik. "Characterization and Differentiation of Kaolinites from Selected Czech Deposits Using Infrared Spectroscopy and Differential Thermal Analysis." 2011.

[41] Kwakye-Awuah, B., E. K. K. Abavare, B. Sefa-Ntiri, I. Nkrumah, E. Von-Kiti, and C. Williams. "Synthesis and Characterization of Geopolymer-Zeolites from Ghanaian Kaolin Samples by Variation of Two Synthesis Parameters." *Journal of Thermal Analysis and Calorimetry* 146 (2021): 1991–2003. https://doi.org/10.1007/s10973-021-10710-9.

[42] Johnson, E. B. G., and S. E. Arshad. "Hydrothermally Synthesized Zeolites Based on Kaolinite: A Review." *Applied Clay Science* 97–98 (2014): 215–221. https://doi.org/10.1016/j.clay.2014.06.005.

[43] Jin, Y., L. Li, Z. Liu, S. Zhu, and D. Wang. "Synthesis and Characterization of Low-Cost Zeolite NaA from Coal Gangue by Hydrothermal Method." *Advanced Powder Technology* 32 (2021): 791–801. https://doi.org/10.1016/j.apt.2021.01.024.